
Electrification of a compact skid-steer loader – redesign of the hydraulic functions

Shaoyang Qu*, Zifan Liu, Rafael Cardoso, Enrique Busquets

Bosch Rexroth, 100 Southchase Blvd, Fountain Inn, SC 29644

* Corresponding author email address: Shaoyang.qu@bosch.com

ABSTRACT

This study introduces an innovative design for the hydraulic implement system in electrified compact loader applications. The presented architecture is based on the pre-compensated load sensing system, incorporating electrified components with energy regeneration capabilities. The system employs an electrified open-center pump (eOC-P) and a load sensing pre-compensated valve sourced from Rexroth. The compensator for the boom function is re-designed to remain static, allowing a bidirectional path for regeneration during the boom lowering phase. The eOC-P offers pressure control, flow control, displacement control, and torque control modes, achieved by replacing the traditional mechanical load sensing feedback with sensor signals. Enhanced by a dedicated control strategy, the re-designed system adapts its operational modes to suit both single and multiple user conditions, aiming to achieve optimal energy performance. This system is designed to seamlessly integrate into the electric drive, reducing components and conserving space in the compact machine, also improving the energy performance. According to the simulation with baseline measurements on a 68kW rated power 5-ton compact loader, the proposed system can save up to 30% energy during a single boom cycle. Moreover, approximately 20% of the input energy can be recovered and stored in the battery, effectively extending the operating hours of the machine.

Keywords: Electrification, Energy regeneration, Load-sensing system.

1. INTRODUCTION

Compact skid-steer loaders stand as key players in the North American machinery market. In response to increased customer interest and more stringent regulations on exhaust emissions, a notable shift towards electrification has emerged within this sector. The electrification concept outlined in this paper includes the removal of the diesel engine and employing electric-hydraulic powertrain for the implement functions. This shift to a purely electric power source addresses emission concern. However, to unlock the full potential of the electrified powertrain, including energy regeneration, a redesign of the hydraulic system and control strategy is imperative.

In the context of compact loader applications, a predominant source of regenerative energy is derived during the boom lowering phase [1]. In traditional hydraulic systems, when the boom moves downwards, potential energy is typically dissipated at the control valve to regulate its lowering speed. This inefficient operation raises a significant challenge for battery-powered machines, impacting their operational longevity [2]. Thus, it is significant to maximize the usage of the regenerative energy for electrified compact loader.

Decentralization is one popular approach to enable energy regeneration. By employing one prime mover for each actuator, the control system can leverage the electric motor – hydraulic pump speed with minimal throttling losses. Additionally, the implementation of a regeneration mode is facilitated through the combination of a hydraulic motor and an electric generator, assuming the hydraulic machine supports two-quadrant operation [3]. The decentralized architecture has demonstrated notable advantages, with reported energy savings of up to 65% [4], and hydraulic efficiency reaching as high as 84% [5] from the previous research by the author. However, it is essential to acknowledge that while decentralized systems offer efficiency gains, they also pose challenges in terms of increased system costs [6]. This is attributed to the necessity of multiple electric and hydraulic machines to cater to all implement functions of the compact loader. To employ one prime mover for multiple functions, the compensated load-sensing (LS) hydraulic system is usually adopted for mobile applications. A cost-effective approach involves employing a single electric machine to directly drive the LS system, providing an intuitive means to control overall expenses [3]. With an electric drive, it becomes feasible to regulate both the drive speed and pump displacement, optimizing energy performance. Research by Lin. T. et al highlights the benefits of an electric load-sensing (e-LS) system, showcasing a reduction of over 20% in energy consumption through an adaptive variable speed and displacement control strategy [7]. However, a limitation of the LS system lies in its prohibition of energy regeneration, as the compensator only permits flow in one direction—from the pump to the actuator—while backflow is essential for energy recovery. Lin. Z. et al investigated the e-LS system and compared energy consumption between centralized LS systems and decentralized e-LS systems, revealing around 12% fuel savings [8]. Despite these efficiency gains, achieving energy regeneration remained elusive in both configurations. A patented hydraulic system uses extra valves on LS systems to enable energy regeneration [9], but not integrated with the electrified powertrain and a dedicated control algorithm as the authors [10].

From the state of the art, the electrification of compact loaders presents inherent trade-offs:

- High costs associated with decentralized architecture, offering enhanced energy performance.
- Absence of energy regeneration and operational inefficiencies with the e-LS system to limit the costs.

This study proposes a novel e-LS system that specifically targets the identified trade-offs. Two pivotal components, the electrified open-center pump (eOC-P) and the modified pre-compensated valve (RM-MPP) sourced from Rexroth, play a crucial role in enabling energy regeneration within the e-LS architecture. A key redesign involves the compensator for the boom function, strategically engineered to remain static, thereby creating a bidirectional path for regeneration during the boom lowering phase. The eOC-P offers pressure control, flow control, displacement control, and torque control modes, accomplished by replacing conventional mechanical load sensing feedback with sensor signals [11]. Consequently, the system attains energy regeneration capability by commanding the eOC-P into motor mode while simultaneously opening the valve section during the boom lowering phase. Through a comprehensive strategy, the proposed system adapts its operational modes based on sensors feedback to accommodate both single and multiple user conditions, with the overarching aim of achieving optimal energy performance.

The structure of this paper is organized as follows: In Section 2, the design and control strategy of the proposed e-LS system are detailed. Section 3 demonstrates the methods for this study, including the simulation model and baseline definition. Section 4 presents the simulation results and corresponding analysis. Finally, Section 5 concludes the study and offers insights into future perspectives.

2. SYSTEM DESIGN

2.1. Reference Vehicle

The reference machine for this study is the Bobcat T770 compact track loader, with the rated power of 68kW, as shown in Figure 1.



Figure 1. Reference vehicle Bobcat T770 compact track loader

Table 1 lists the key parameters of the reference machine. It is important to note that in the context of this electrification study, the diesel engine, along with all hydraulic and thermal components, has been eliminated from the reference machine. This commercial compact loader establishes the sizing requirements but also serves as the benchmark for achieving the performance targets outlined in the electrification proof of concept.

Table 1: Main specifications of the reference vehicle

<i>Specifications</i>	<i>Values</i>
Engine Type	3.4L Bobcat Diesel Engine, 4 cylinders
Max power	92 hp [68 kW]
Max Standard flow	23 gpm [87 L/min]
Machine Weight	10,515 lb [4770 Kg]

Engine speed	1100-2600 rpm
--------------	---------------

This paper focuses on the control of two crucial implement functions of the vehicle, boom and bucket actuation. Figure 2 provides the parameters associated with these functions. The reference machine utilizes conventional pre-compensated LS system for its implement functions. Based on the actuation data, the electrified hydraulic system undergoes a redesign, with components sized to meet the demands of the original cycle requests.

Table 2: Parameters of the boom and bucket actuators.

<i>Actuation parameters</i>		<i>Value [unit]</i>
Boom cylinder and cycle time	Length of stroke L_{boom}	662.7 [mm]
	Diameter of piston D_{boom}	82.6 [mm]
	Diameter of rod d_{boom}	50.8 [mm]
	Raising arm time $t_{boom,ex}$	4.8 [s]
	Lowering arm time $t_{boom,re}$	3.4 [s]
Bucket cylinder and cycle time	Length of stroke L_{bucket}	349.0 [mm]
	Diameter of piston D_{bucket}	76.2 [mm]
	Diameter of rod d_{bucket}	38.1 [mm]
	Bucket dump time $t_{bucket,ex}$	2.34 [s]
	Bucket rollback time $t_{bucket,re}$	2.05 [s]

2.2. Proposed System

Figure 2 presents the hydraulic schematic of the implement system for the electrified tracked loader. For the sake of simplification and to maintain focus on the study's scope, certain elements such as the auxiliary section and functions like parking brake control are excluded from the illustration. The proposed architecture incorporates key components, including the eLION inverter and electric motor as the prime mover, the A10VO eOC unit capable of 4-quadrant operation, and the RM pre-compensated LS valve. Notably, the boom control section is enhanced with a static compensator, a modification crucial for enabling energy regeneration. The modification on the compensator with an extra shim to keep it open statically, but this valve section is still capable with other RM sections without any change on the platform. The schematic emphasizes the inclusion of essential sensors, such as pressure sensors, displacement sensors at the actuators, and the angle sensor of the eOC-P. These sensors play a vital role in providing feedback necessary for effective control.

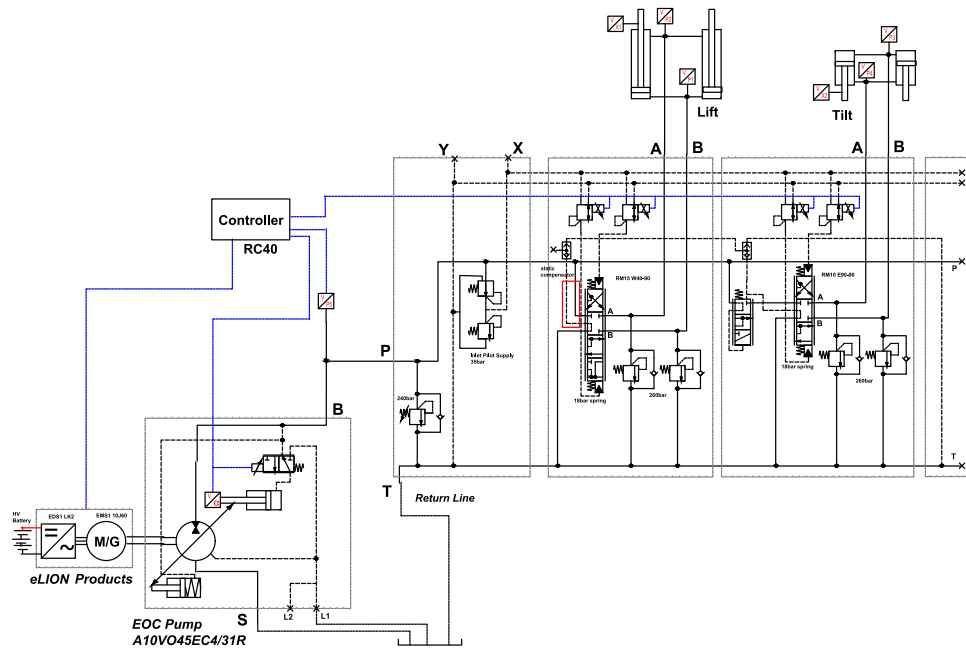


Figure 2. Hydraulic schematic of the proposed system

Figure 3 provides a visual representation of the working principle behind boom control with energy regeneration. The modification of the compensator to a static, always wide-open configuration allows for the implementation of displacement control for the boom function with the eOC-P capable of 2-quadrant operation, which covers both positive and negative displacement. The velocity of the boom actuation is governed by the pump displacement α , dictating the flow rate Q to the system in both directions. Simultaneously, this controls the power flow P to the electric machine and inverter, assuming an unchanged shaft speed. Notably, the valve can be fully opened, a design feature that serves to minimize throttling losses.

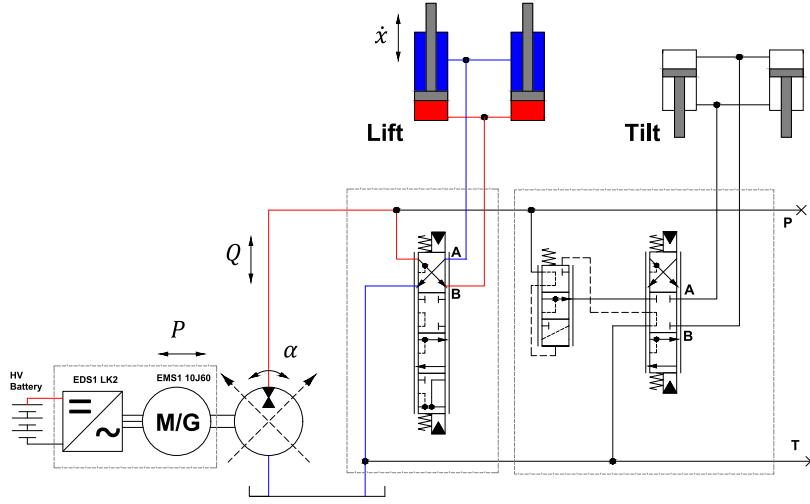


Figure 3. Regeneration capability from the boom function

The flow rate delivered to the boom actuators is as equation (1), where V_d is the maximum displacement of the pump.

$$Q = n \cdot V_d \cdot \alpha \cdot \eta_{vol} \quad (1)$$

And the velocity of the boom cylinders follows equation (2). Thus, the velocity can be controlled by adjusting the pump ratio α as given in equation (3). The ratio α could be negative for regeneration mode when the boom cylinders retract with negative \dot{x} too.

$$\dot{x} = \frac{Q}{2 \cdot A_{boom}} = \frac{Q}{2 \cdot \pi D_{boom}^2} \quad (2)$$

$$\dot{x} = \frac{n \cdot V_d \cdot \alpha \cdot \eta_{vol}}{2 \cdot \pi D_{boom}^2} \quad (3)$$

While the example above focuses on boom control in a single-user scenario, the introduced modifications in the LS architecture pose a control challenge when considering multiple-user conditions. Consequently, a novel control strategy is proposed to address this complexity.

2.3. Control Strategy

Figure 4 illustrates one multiple user condition, wherein both the boom operation and bucket rollback occur at the same time. The compensator of the bucket section regulates the flow rate to the bucket cylinders Q_j , and the pump output flow can be controlled using equation (1). As a result, the flow rate to the boom cylinders is derived as $Q_p - Q_j$. If the user requires Q_i for the boom, the pump flow is controlled according to equation (4). In contrast to the conventional LS system, the proposed system eliminates the need for a boom compensator, replacing its functionality by directly controlling the pump flow using the eOC-P. Other functions with compensators maintain the same control principles.

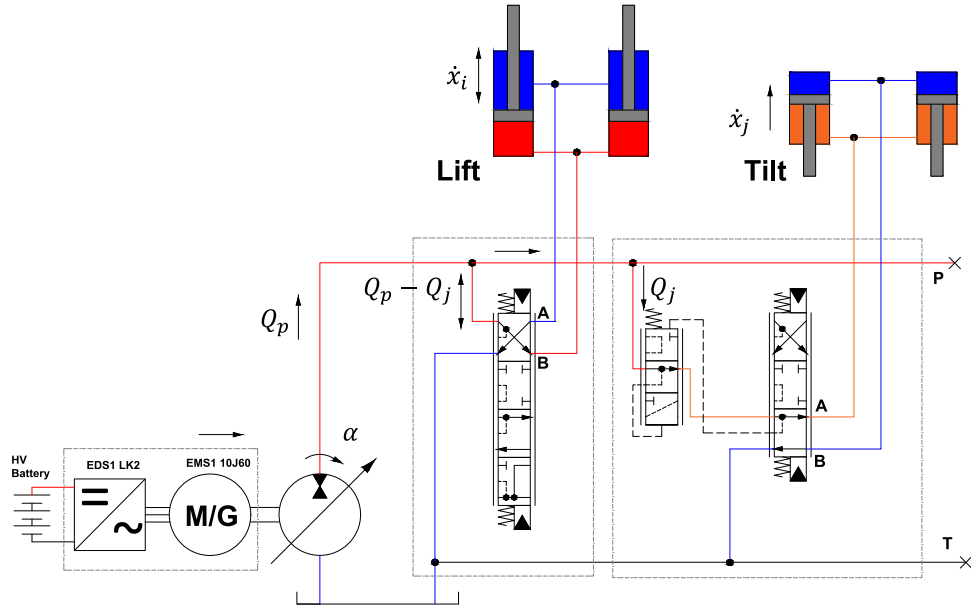


Figure 4. Control strategy for multiple users boom and bucket.

$$Q_p = Q_i + Q_j \quad (4)$$

One fact about this tracked loader application is that the load pressure of the boom cylinder p_i tends to be higher than that of the bucket cylinder p_j . Under this scenario, the valve for boom control can be fully opened to optimize efficiency, given that the flow typically aligns with the requests of the compensated bucket function, which operates at a lower pressure. Energy regeneration is feasible when $p_i > p_j$ when lowering the boom, utilizing backflow from the boom to fulfill the bucket's needs. The eOC-P would provide the rest of required flow. Conversely, if $p_i < p_j$, metering control of the boom valve may be applied to meet flow requests during the boom-raising phase. In instances where energy regeneration is not possible during boom lowering, the boom valve section can switch to the PA position, as depicted in Figure 5. The control principle is the same with Figure 4, but this scenario excludes energy regeneration due to the necessity for high pressure during downward boom movements, like in some piling operation. The mode presented in Figure 5 is similar to the conventional LS control in terms of overrunning the boom down but not regenerating from this operation phase.

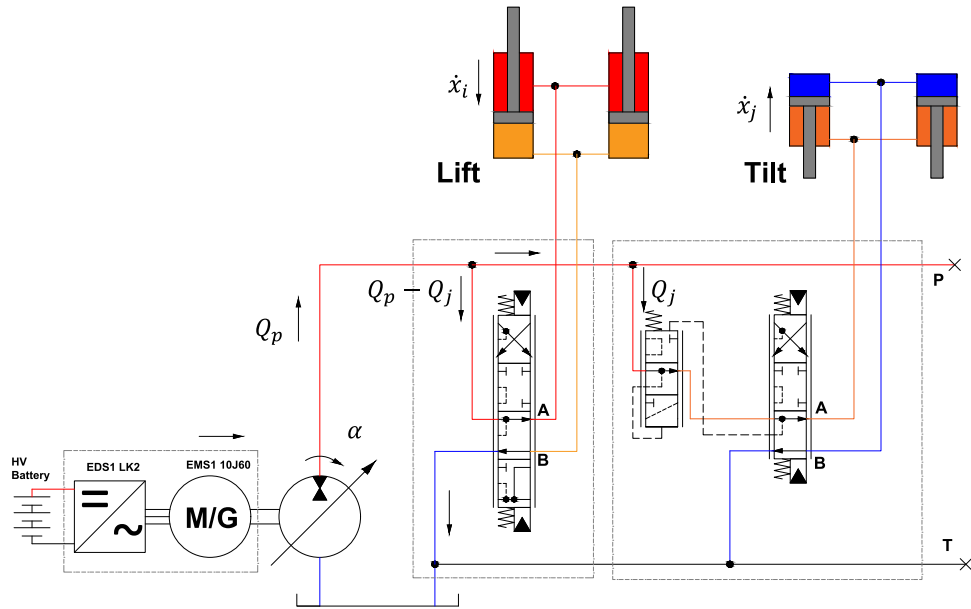


Figure 5. Control strategy for multiple users, lowering the boom without energy recovery.

An alternative method to control the boom lowering involves employing the float section of the valve, as presented in Figure 6. In this scenario, the flow control of the boom floating operates independently of the bucket control. This mode proves advantageous in situations where the load pressure of the boom is low, and energy regeneration is not attainable.

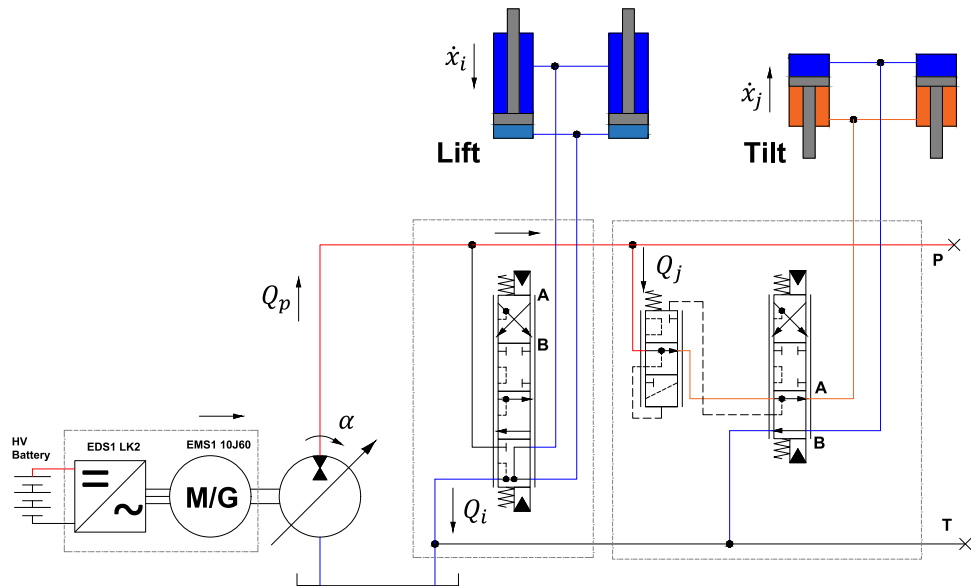


Figure 6. Floating mode of the boom control.

The control strategy is summarized in the flow chart presented in Figure 7. For single-user cases, employing displacement control for the boom is a straightforward approach, facilitating energy regeneration during boom operation. For multiple-user conditions, the compensator associated with the bucket regulates the flow rate along its path, while the pump delivers the required flow for all functions. Under different loading conditions with feedbacks from the sensors, the controller would switch the boom valve position, aiming to fulfil the functionality with optimal energy performance. Additionally, the boom section includes a float position designed for lowering the boom under specific conditions.

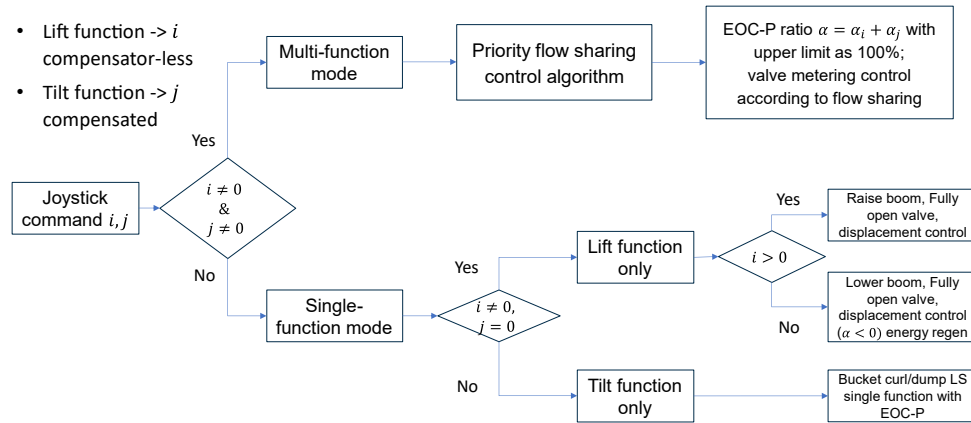


Figure 7. Flow chart of the control strategy for the proposed architecture.

3. METHODS

This study adapts both experimental and simulation methods. Initially, the baseline was established through on-field measurements with the reference machine. From the baseline data, a sizing study was conducted to choose suitable components for the proposed system, including the electric machine, hydraulic machine and valves. Subsequently, a lumped-parameter model was developed within AMESIM environment, with specifications of the chosen components as parameters, and baseline data as the model inputs. The simulation model incorporates the efficiency map of the pump and dynamic behaviours of the valves, creating a realistic environment for simulating and fine-tuning the control strategy in preparation for the vehicle demonstration. At present, the proposed system has been installed on the electrified compact loader, and ongoing tests are in progress. Therefore, this paper will focus on presenting simulation results.

3.1. Baseline and setup

Figure 8 presents a picture of the ongoing baseline measurements, undertaken at the test field at Bosch Rexroth in Fountain Inn, South Carolina. Various operating conditions were tested, such as fast traveling, Y-cycle, gradeability, etc. Specifically, the Y-cycle data obtained during these measurements serves as both a reference and inputs for the simulation of the hydraulic implement system.



Figure 8. Baseline measurements on the reference machine, Y-cycle operation.

The selected components and product number of those are listed in Table 3, including the Rexroth eLION products, eOC-P and the RM-MMP valve platform.

Table 3: Selected components for the proposed electrified system

<i>Component</i>	<i>Product Number</i>
Electric machine	EMS1-10J60LM7-RSCB-W1M7NNNNN
Inverter	EDS1-L0400 KNN-12 ECNM1RDNN-S03RSN9
Hydraulic machine	A10VO0045 EC4 000PL3/60DL VB2
Valve inlet plate	M4-12-2X / J 260 Y
Boom section	RM15 S1 S22ZZZ W040-090 H24H24 S00
Bucket section	RM10 S1 S22ZZZ E090-090 H24H24 S00
Auxiliary section	RM15 S1 S22ZZZ E110-110 H24H24 S00
Valve end plate	M4-12-2X / LA
Pressure sensors	PR4 280 U7 D SE/10, PR4 050 U7 D SE/10
Parking brake valve	SV08-30-6T-N-24ER
Oil filter	50LE0150-H10XLA00-V2,2-M

3.2. *Simulation model*

A lumped-parameter model was developed in AMESIM environment as depicted in Figure 9, it is evident that the architecture of the model aligns with the schematic illustrated in

Figure 2. The selected components have their parameters determined using measured data, ensuring the model reflects realistic performance to the maximum extent. These parameters include the efficiency map and simplified controller of the eOC-P, flow curves with pressure drops associated with the RM valve, and the lookup table of the load force derived from the Y-cycle baseline measurements. The primary outputs of the simulation focus on functionality within the compensator-less design and energy performance.

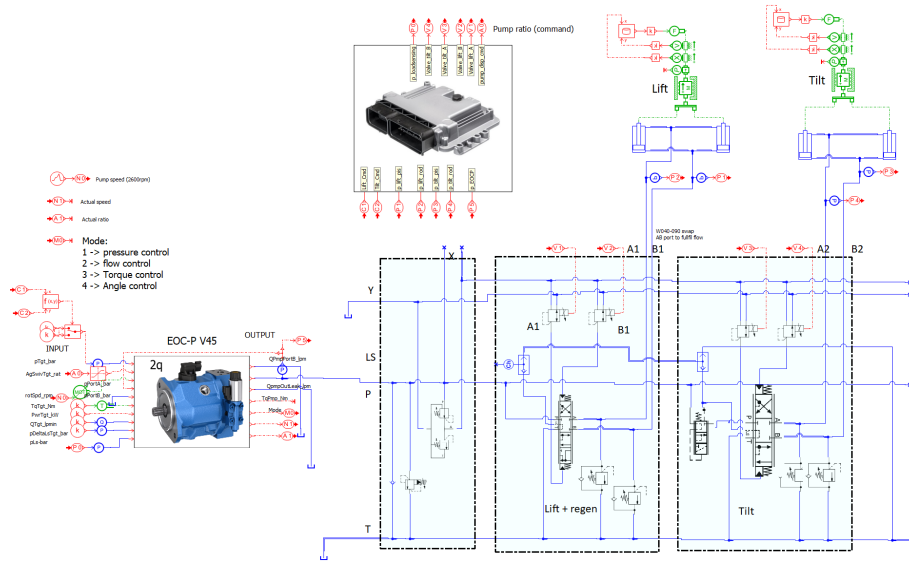


Figure 9. AMESIM simulation model of the electrified implement system.

4. RESULTS

4.1. Sizing study

Figure 10 represents the load force table of the boom actuators generated from the baseline data. During the boom up and down cycles, the load force F applied to the actuators is related to the displacement and the velocity. Equation (5) defines this relationship using measured pressures p_{pis} , p_{rod} at the piston and rod sides. The displacement alters the act angle between the actuators and the mechanism, consequently impacting the load force. In the case of the boom, an increase in displacement aligns the actuators more vertically, resulting in a decrease in load force. The velocity is related to the mechanism friction. When raising the boom, higher velocity leads to greater friction opposing the boom actuators, resulting in an increase in load force. Conversely, during boom lowering, the friction opposes in the opposite direction, causing a decrease in load force. These tables for boom and bucket work as the inputs of the AMESIM simulation model. The loading condition also provides reference for the sizing of the components.

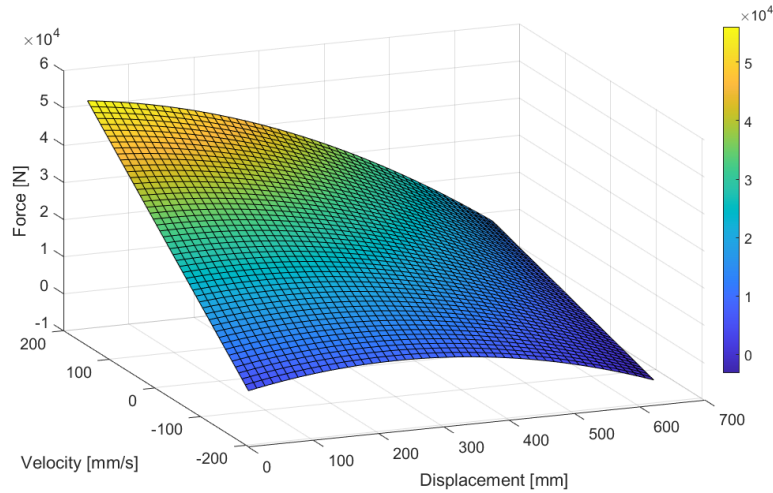


Figure 10. Load table generated from the baseline measurements, boom Y-cycle operation.

$$F = p_{pis} \cdot \pi D^2 - p_{rod} \cdot \pi(D^2 - d^2) \quad (5)$$

Figure 11 demonstrates the sizing considerations for the electric machine regarding the speed and torque performance. For electric machines, two curves serve as reference points: the continuous curve and the peak curve. The electric motor can run under the continuous line without limits. However, if the operation exceeds this curve, additional cooling measures may be necessary. The orange peak curve, indicating the limit for a 60-second duration, sets the boundary for operations beyond the continuous curve.

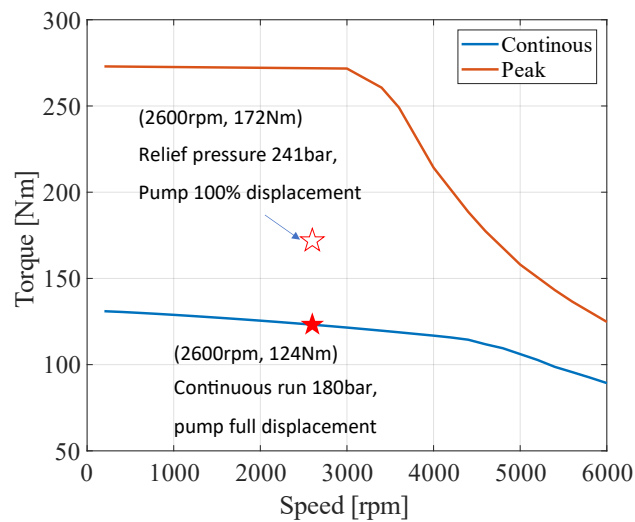


Figure 11. Sizing of the electric machine, EMS1-10J60 speed and torque curve

To select the proper electric machine for hydraulic implements often revolves around the consideration of maximum torque. The peak torque T of the hydraulic machine can be obtained using equation (6), where dp is the maximum pressure difference. Assumed relief pressure as dp and full displacement of the pump, the torque will reach the theoretical peak value. This point falls between the peak and continuous curve depicted in Figure 11 to avoid oversizing. Operating at continuous torque, the pump can function at 180bar with full displacement, or at relief pressure with about 75% displacement. This configuration aligns with operational requirements based on the baseline data.

$$T = dp \cdot \frac{V_d}{2\pi} \cdot \frac{1}{\eta_{mh}} \quad (6)$$

In terms of efficiency of the proposed system, the energy losses of the electric machine and inverter are not included in this study. Thus, the comparison is mainly about the hydraulic system.

4.2. *Simulation results*

Figure 12 represents an example of the AMESIM simulation results, capturing a complete boom raising and lowering cycle, like the mode illustrated in Figure 3. The first plot showcases the boom command and displacement, while the second provides the eOC-P ratio and the load pressure at the boom cylinder piston side. The third plot displays the power and energy consumption of the hydraulic systems, calculated at the pump shaft.

From the plots, the boom raising phase extends from 1s to approximately 6s, followed by the initiation of the lowering phase around 7s, persisting for about 4s. Notably, between the two black lines around 7s to 8s, the low load pressure disabled the energy regeneration, activating the float function to lower the boom instead, as indicated in Figure 6. The system requires a minimum of 18bar for pilot control, meaning energy regeneration is only enabled if the load pressure exceeds this threshold. Beginning at 8s, the ratio of the eOC unit becomes negative and works as a motor, energy regeneration starts and the power flow reverses direction as indicated in the third plot, until the cycle ends at about 11s.

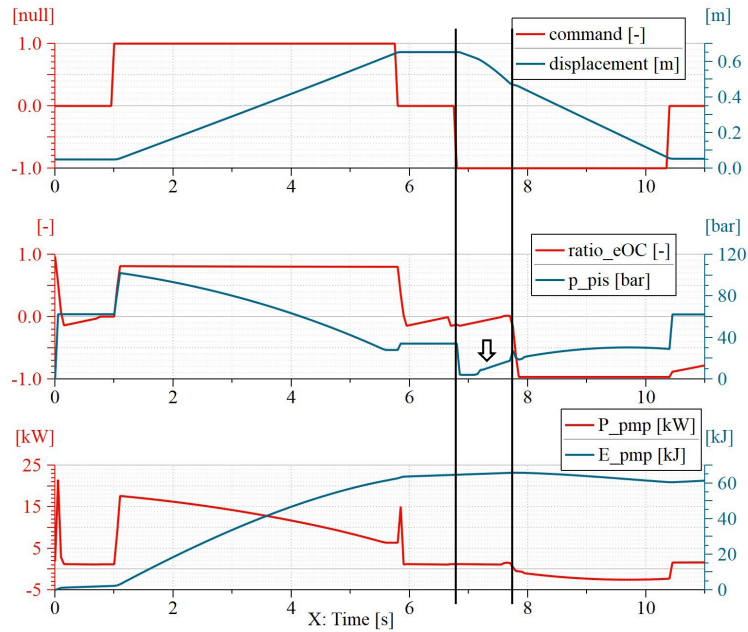


Figure 12. Simulation of one boom cycle with energy regeneration

For comparison, Figure 13 demonstrates the power and energy consumption in the cycle represented in Figure 12, where the speed command and actual displacement are presented. The baseline is the LS system with standard RM valves with loading conditions from the measurements on the vehicle, so the results should indicate the benefits from the energy regeneration with the electrified powertrain and modified compensator. Comparing the power consumption, the proposed electrified system saves energy during the lowering phase by regeneration. Moreover, because of its compensator-less design, the proposed architecture minimizes the throttling losses and additional energy saving is achieved during the raising phase as well. At approximately 7s, the baseline system experiences an extra power consumption spike due to insufficient load pressure at the piston side for assistive operation.

Regarding the energy consumption during one boom cycle, as depicted in the second plot, the baseline system records 90.4 kJ compared to the proposed system's 61.4 kJ, translating to a remarkable **32% energy saving** compared to the baseline system.

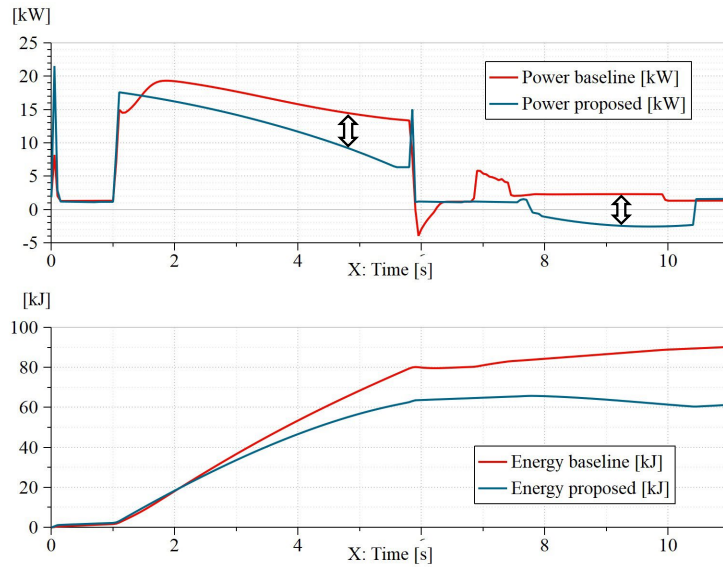


Figure 13. Power consumption comparison from the simulation

For multiple user conditions, Figure 14 represents the results with boom and bucket Y cycle operation. The first plot provides an overview of the cycle commands, with both actuators being commanded during the time slots of 2s-4s and 6.5s-7.5s. The second plot illustrates the displacement of the actuators, while the third plot presents the ratio of the eOC-P, offering insights into the flow control dynamics of the system.

During the period from 2s to 4s, the system operates in the control mode depicted in Figure 4. The pump is tasked with supplying the required flow for both the boom and the bucket. If the pump ratio reaches 100%, a flow sharing condition occurs, as seen between 3s to 4s. In this instance, an increased command to the bucket results in a decrease in the boom velocity. While this paper does not delve into specific control algorithms addressing flow sharing conditions based on user priority, it remains an option for further refinement. From 7s-7.5s, the boom drops down and the bucket rolls back. Throughout this time slot, the ratio of the eOC-P remains positive, indicating no energy regeneration with the bucket load pressure higher than that of the boom cylinders. After 7.5s, the system transitions into regeneration mode, specifically with boom lowering, causing the pump ratio to change to a negative value.

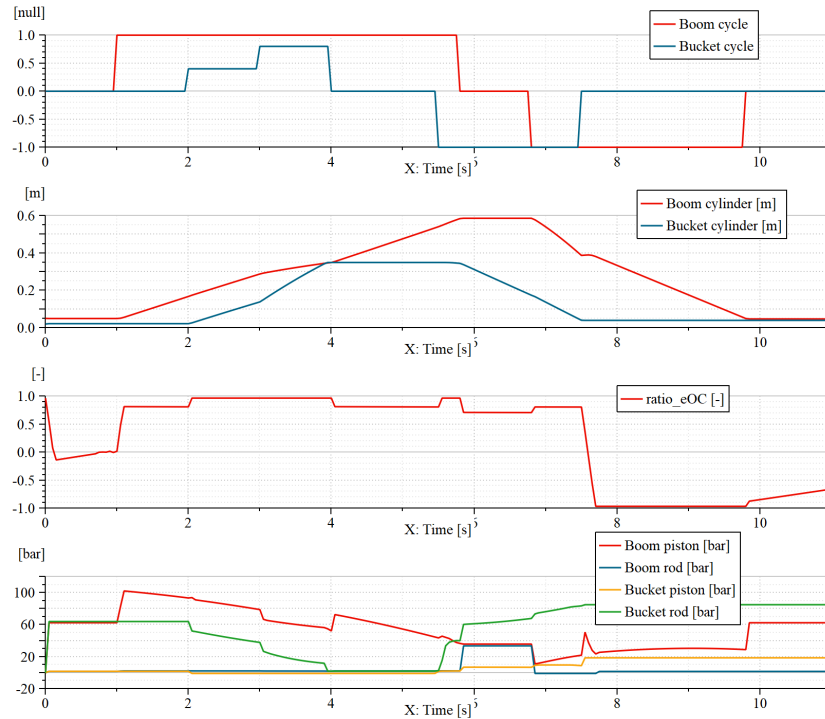


Figure 14. Simulation of the multiple user case, boom and bucket Y cycle operation

5. CONCLUSION

In this study, we introduced an innovative electrified hydraulic implement system based on conventional LS architecture. The modification of the boom function's compensator to a static state facilitates energy regeneration, and a corresponding control strategy has been devised. This strategy employs the capability of the eOC unit, incorporating displacement control and motoring mode to effectively address the complexities associated with multiple user conditions.

To investigate the proposed system, baseline measurements have been conducted on the reference compact track loader, leading to the selection of suitable components through a comprehensive sizing study. Subsequently, a lumped parameter model was developed in AMESIM environment. With the components' specifications and the measured loading conditions as the inputs, the simulation can reflect the realistic working conditions. The boom cycle simulation validates the displacement control strategy, revealing a remarkable energy savings of over 30% compared to the baseline LS system. Simulation results for multiple user conditions further explore various working modes as proposed, affirming the effectiveness of the control strategy.

As of now, tests on the proposed system are ongoing on the demonstration vehicle, and the gathering of additional data will contribute to refining the controller design, particularly in terms of dynamic behavior and handling extreme conditions. These ongoing tests aim to further enhance the overall performance and robustness of the proposed electrified hydraulic implement system.

REFERENCES

- [1] Lin, T., Lin, Y., Ren, H., Chen, H., Chen, Q., & Li, Z. (2020). Development and key technologies of pure electric construction machinery. *Renewable and Sustainable Energy Reviews*, 132, 110080.
- [2] Lin, T., Chen, Q., Ren, H., Huang, W., Chen, Q., & Fu, S. (2017). Review of boom potential energy regeneration technology for hydraulic construction machinery. *Renewable and Sustainable Energy Reviews*, 79, 358-371.
- [3] Fassbender, D., Zakharov, V., & Minav, T. (2021). Utilization of electric prime movers in hydraulic heavy-duty-mobile-machine implement systems. *Automation in Construction*, 132, 103964.
- [4] Qu, S., Zappaterra, F., Vacca, A., & Busquets, E. (2023). An electrified boom actuation system with energy regeneration capability driven by a novel electro-hydraulic unit. *Energy Conversion and Management*, 293, 117443.
- [5] Qu, S., Fassbender, D., Vacca, A., & Busquets, E. (2021). A high-efficient solution for electro-hydraulic actuators with energy regeneration capability. *Energy*, 216, 119291.
- [6] Qu, S., Fassbender, D., Vacca, A., & Busquets, E. (2021). A cost-effective electro-hydraulic actuator solution with open circuit architecture. *International Journal of Fluid Power*, 22(2).
- [7] Lin, T., Lin, Y., Ren, H., Chen, H., Li, Z., & Chen, Q. (2021). A double variable control load sensing system for electric hydraulic excavator. *Energy*, 223, 119999.
- [8] Lin, Z., Lin, Z., Wang, F., & Xu, B. (2024). A series electric hybrid wheel loader powertrain with independent electric load-sensing system. *Energy*, 286, 129497.
- [9] WO24058689-A1, Hydraulic System, Lejonberg Robert, Maennistoe Ville, (2024). International patent
- [10] US patent, E-Load sensing system with compensator-less design, Shaoyang Qu, Rafael Cardoso, Enrique Busquets, (2024), in process.
- [11] US2021025414 (AA) - Hydraulic Pressurizing Medium Supply Assembly, Method, And Mobile Work Machine EOC patent, Geiger Daniel, Muehlbauer Florian, Golde Marcel, Brand Michael, An Minha, Tetik Salih, Wang Ximing, (2021)